



Cite this: *Mater. Adv.*, 2024, 5, 5036

Received 1st March 2024,
Accepted 21st May 2024

DOI: 10.1039/d4ma00210e

rsc.li/materials-advances

What makes cements bind?—A proposal for a universal factor

Hoang Nguyen * and Paivo Kinnunen

The cement industry needs radical solutions to reduce its carbon emissions. Here, we look at the fundamental question about the cohesion of cement, and give our perspectives on an overlooked factor: the amorphicity of cement reaction products. We discuss how the amorphicity can enable a scientifically-guided strategy to design and realize novel cements. Through this work, we invite the research community and cement scientists to unveil common principle(s) behind the cohesion of not only conventional Portland cement but also other emerging low-carbon cements. By adding this factor to the design framework for cement, we may radically enhance the progress of decarbonizing the industry while using less but achieving more in producing cements and concretes.

Introduction

The cement industry has been one of the major emitters accounting for 6–8% of anthropogenic CO₂ emissions.¹ It is the second most used material on Earth after water and the largest manufactured product by mass. The current production of Portland cement (*i.e.*, the major and most dominant type of cement) is *ca.* 4 Gt year⁻¹ worldwide and with the increase in the human population, its demand will keep raising and is forecasted to reach *ca.* 6 billion tons per annum in 2050.² This leads to an urgent need to decarbonize the industry with sustainable-by-design solutions. Among these solutions, the more efficient use of cement without compromising the performance of end products has been a strong focus of both academic research and industrial practices.

To produce a concrete, cement acts as a “glue” phase to bind aggregates of different sizes, thus giving strength to the concrete once it is hardened. When zooming in on the process, Portland cement hydration consists of the hydration of different clinker phases including alite (C₃S—Ca₃SiO₅) and belite (β-C₂S—Ca₂SiO₄), leading to the formation of calcium silicate hydrate (CSH).³ CSH is a nanocrystalline phase (Fig. 1) with variable compositions including different Ca/Si ratios and alkali/aluminate uptakes. The formation and growth of this nanocrystalline phase drives the strength development of the concrete structure. Through the lens of micromechanics with the gel-space ratio⁴ (*i.e.*, the ratio of the volume of hydrates to the volume of both hydrates and capillary pores), cement paste is a composite of a matrix of CSH with cement clinkers as reinforcements.

Fibre and Particle Engineering Research Unit, University of Oulu, Pentti Kaiterankatu 1, 90014 Oulu, Finland. E-mail: Hoang.Nguyen@oulu.fi, Paivo.Kinnunen@oulu.fi

Sharing similar principles with Portland cement, emerging and alternative low-carbon cements have been reported and their mechanical performance is often based on nanocrystalline/amorphous phases as well (Fig. 1). However, little is known about the cohesion in alternative cements and it remains unclear what are the driving forces of cohesiveness in these cements. In addition, although the literature about cohesion in Portland cement is rather comprehensive, the nature of cohesiveness of CSH is still a matter of debate (detailed in the next session). Therefore, motivated by the need to design better

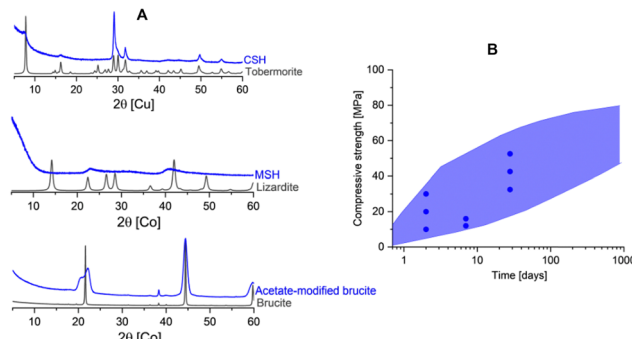


Fig. 1 (A) The amorphicity of binding phases compared to their crystalline counterparts: C(A)SH in Portland cement and alkali activated cement vs. tobermorite;⁵ MSH⁶ in magnesium silicate cement vs. lizardite.⁷ We show here one example [unpublished data] where we steered the hydration of MgO to form low-crystalline brucite using acetate ligands, which in turn provide promising mechanical strength compared to crystalline brucite. This distorted brucite shared similar characteristics with the hydrous carbonate-containing brucite as found in magnesium carbonate cement. (B) The common range of strength and its development in several major and emerging cements where the dots represent the expected strength in Portland cements as regulated in EN 197 standards. In contrast, the crystalline counterparts do not show such strength development.

cements it has been attracting our interests to address the fundamental question: "What makes cements bind?". Ideally, we would hope to discover common principle(s) of cohesion behind emerging cements and conventional Portland cement. By better understanding factors that lead to cement cohesion, one can design cements in which increased performance can be achieved while using less resources and with lower carbon footprint.

Here, we give our perspective about an overlooked factor in cement that can be used as a predictor of cohesion potential of cement—lack of long-range order or in a word 'amorphicity' of the reaction products. We make the case for it to be a powerful predictor for cement performance that can be used to design novel cement chemistries. We also provide our perspective of how it enables a scientifically-guided strategy to be able to use less but achieve more in producing concrete.

Current paradigm of cement cohesion

In this section, we will summarize the current paradigm of Portland cement cohesion, which is driven by CSH phase. The cohesion has been understood through a complex relationship between interfacial strength and surface charge among CSH particles as well as factors known to affect the cohesion. Here, we take CSH as the model since the open literature has little information about the cohesiveness of other types of cements.

Interfacial strength between CSH particles

Closely contacted CSH particles are the key to give bulk strength rather than the total porosity (Fig. 2). Zhang *et al.* found that CSH powder could develop strength when compressed under high pressure.⁸ In the presence of excessive water between CSH particles, the bond is clearly weakened. Under molecule-level modeling, Duque-Redondo *et al.*⁹ showed that the cohesion of CSH relies on the interfacial distance, and its water content among nano-sized CSH particles and their layers. The loss of cohesion in CSH was linked to the water mobility in CSH, which led to the increase in the interlayer distance. Therefore, the cohesion of CSH was shown to connect with the interfacial properties among CSH particles which led to strength-gain in the hardened cement as well as long-term properties such as creep.

Charged surfaces of CSH

In an effort to control the cohesion of cement paste, Jönsson *et al.*¹⁰ found two main factors that control cohesion: the surface charge density and the valency of the counterions. In addition, the cement cohesion was not affected by the addition of a large variety of additives showing that the calcium concentration and the CSH surface charge were high enough.

More recently, Goyal *et al.* found that during the formation of CSH, ions and water get progressively confined between increasingly charged surfaces of cement hydrates (Fig. 3).¹¹ This leads to a change in ion-water interlocked structures and their stability, which in turn, alters the net pressure between CSH surfaces as hydration proceeds. The change in nanoscale

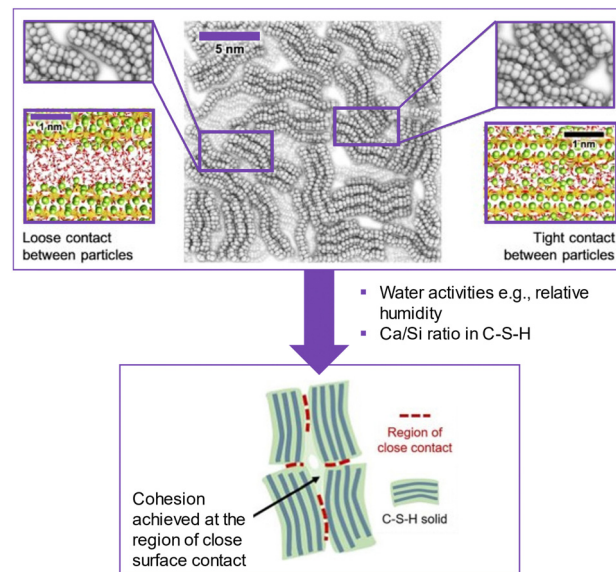


Fig. 2 Schematic picture of the nanoscale structure of the CSH gel (center). In the top-left and -right, the magnifications show two possible interparticle interfaces: a loose (left) and tight (right) contact. The close contact among CSH particles contributed to the strength of the CSH pellet as seen in the developed case in ref. 8 (reproduced from ref. 8 and 9 with permission from Elsevier, copyright 2022).

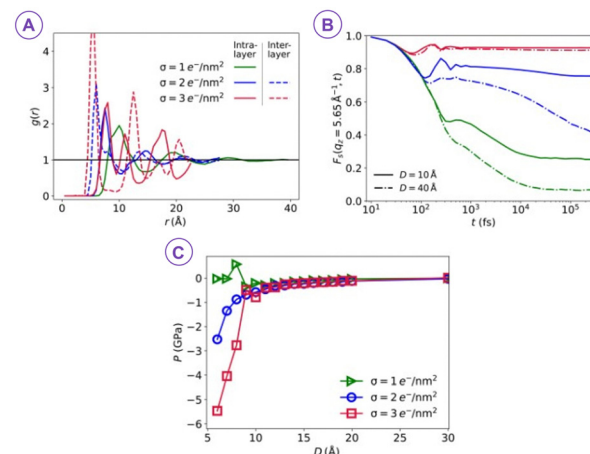


Fig. 3 (A) The xy pair correlation $g(r)$ between ions indicates that as the surface charge densities σ increase at fixed separation $D = 8 \text{ \AA}$, ions become closer together and their positions become more correlated. (B) Intermediate scattering functions $F_s(q_z, t)$ for the ions measured for the same σ values as in (A) and for two different surface separations $D = 10$ and 40 \AA . Here, the stronger spatial correlations with increasing surface charge density in (A) correspond to increasingly correlated dynamics and more strongly localized ions. (C) The increasing correlations drive the overall pressure between the confining walls to become increasingly attractive, reaching $P_{\min} \simeq -6 \text{ GPa}$ at $\sigma = 3 e^- \text{ nm}^{-2}$ (reproduced from ref. 11 with permission from AAAS, copyright 2021).

interactions, characterized by competing attraction and repulsion, and the enhanced attraction strength with increasing surface charge density during hydration, play a significant role in shaping the morphology of mesoscale structures forming the



gel network. This builds the gel network and can markedly steer compressive or tensile stresses along with the progression of the hydration *via* densification and solidification.

Two major factors affecting CSH cohesion

The two major factors that affect the CSH cohesion include the Ca/Si ratio and water content in the CSH phase. The former was seen to increase the cohesion of CSH when increasing the Ca/Si ratio.¹² However, contrasting observation has been reported at the macro scale where the compressive strengths of the CSH pastes increase when the Ca/Si ratio decreases at different testing ages.¹³ On the other hand, the increase of water content is found to decrease the cohesion of CSH. Water also has a detrimental effect on the viscous properties of the phase.¹²

Amorphicity—an overlooked factor toward a better design for cements

Now, we know that the current paradigm of cement cohesion is based on interfacial strength and charged surfaces of CSH and that the relationship and the dynamics between the two remain unclear. Furthermore, literature to date explains dynamics in CSH systems, but the models do not generalize to other chemistries readily and therefore have limited predictive power in terms of conceiving novel cements. However, both models take for granted the highly amorphous nature of the binder; the crystalline counterpart of CSH is non-binding tobermorite. Plus, we see the same pattern in other types of cements where binding phases in these cements share similarity in the amorphicity.

Binding phases in different cements

In Portland cement, CSH is the major binding phase with a poorly ordered structure which relates to a defective 11 Å tobermorite structure. The structure of 11 Å tobermorite⁵ is considered to be a crystalline counterpart of CSH in which the mineral consists of infinite layers of CaO polyhedra with tetrahedral silicate chains on both sides of the layers.¹⁴ The silicate chains are negatively charged, which is compensated by additional Ca²⁺ in the interlayer. In contrast, CSH gel exhibits a disordered structure *e.g.*, the absence of cross-linked bridging sites,¹⁵ turbostratic stacking,¹⁶ and the ability to uptake alkalis and Al.¹⁷ The flexibility in CSH structure leads to a wide range of different X-ray amorphous CSH compositions and eventually gives major contributions to strength development of Portland cement.

In alkali-activated cement, an amorphous Al-tobermorite-like gel accounts for the strength. Notably, the CASH gel formed in this class of cement differs from the CSH produced by Portland cement hydration. This is mainly attributed to the low Ca/Si ratio and high Al content of the gel produced by alkali activation of blast furnace slag, which opens up the possibility of cross-linking between the dreierketten chains of the tobermorite-like gel.¹⁸ When the system is short in Ca, NASH gel may form after the alkali activation and is often called

geopolymer.¹⁹ The NASH gel is considered to have an X-ray amorphous zeolite structure.¹⁹

Other emerging low-carbon cements share similar nature in terms of amorphicity of the binding phases. Magnesia-based cements offer a conceivable solution to decarbonize the cement industry due to their potential for low-to-negative CO₂ emissions.²⁰ The two major MgO-based cements include magnesium silicate and magnesium carbonate cement. The former binds based on magnesium silicate hydrate (MSH)²¹ while hydrous carbonate-containing brucite²² accounts for the binding in the latter. MSH has an amorphous (nanocrystalline) layered silicate structure with tetrahedral layers as in phyllosilicate minerals.^{6,23} Therefore, MSH is considered to be a complex composite-like phase consisting of multiple amorphous hydrate magnesium silicate phases²⁴ whereas its crystalline counterparts can be Mg-silicate minerals such as sepiolite and lizardite⁷ with no binding capacity. As for magnesium carbonate cement, the hydrous carbonate-containing brucite (HCB) is a defective (*i.e.*, amorphous) brucite which results from stacking faults occurring during the hydration of MgO in the presence of (bi)carbonates.²⁵ We also found that stacking faults can also be done in the presence of acetate,²⁶ which strongly influences the binding properties of acetate-modified brucite. While the crystalline brucite shows limited strength-giving performance, this carbonate or acetated-defected amorphous brucite shows comparable binding properties to conventional Portland cement.^{22,27}

In all the five examples (CSH, CASH, NASH, MSH and HCB) we see the same trend: cementitious binding phases are amorphous counterparts of stable non-binding crystalline minerals. One could argue the same is the case also for ettringite-based binders^{28,29} [with low-crystallinity AFm phases and Al(OH)₃] and calcium aluminate cements [with metastable calcium aluminate hydrates and Al(OH)₃.³⁰ The fact that all cements share this property seems to indicate that they actually bind due to the amorphicity of their formed phases. In short, implicit in the current paradigm is the assumption that whatever makes cement bind is amorphous in nature. Yet, we have a counterexample to be discussed.

Counterexample—the case of magnesium phosphate cement

Magnesium potassium phosphate cement hardens based on the acid-base reaction between KH₂PO₄ and MgO. The cement exhibits several outstanding engineering properties including fast setting and high-early compressive strength. The performance of this cement is known to come from a complex formation of various phases in the MgO-KH₂PO₄-H₂O system and the majority of the phases are crystalline.³¹ Therefore, it is of interest to know whether other driving forces take place in this cement and what synergy among these crystalline phases there is.

However, when taking a closer look at this system, there are indicators that amorphous magnesium phosphate exist and may play a role as well.^{32,33} Therefore, it will be important to better understand the reaction mechanism in the magnesium potassium phosphate cement and relationship among phases



including the nature of these amorphous phases and whether they contribute to the binding properties. Here, we are open for further discussion on the case of this cement and look forward to more in-depth understanding about their binding phase.

Why does it matter?

Amorphicity can be defined in a variety of ways, and can mean slightly different things, and what we mean here is X-ray amorphicity. Specifically, any material producing non-sharp XRD reflections, which we interpret to mean that the material does not have a periodic structure in one or more diffracting directions and is therefore amorphous. Therefore, amorphicity is simple to measure and seems to capture the main requirements for turning a stable mineral into an interesting cementitious binder regardless of whether the binding occurs *via* charged surfaces, interfacial bonding among particles or by the 3D network of covalent bonds. In practice, some cements may solely contain or blend with amorphous precursors (*e.g.*, glassy alumino silicates^{34–36}), and other characterization tools (*e.g.*, NMR and PONKS³⁷) are desirable to couple with XRD to distinguish these cementitious precursors from amorphous hydrates and also achieve fuller understanding about reactions in these cements.

Amorphicity as a concept is also powerful because it bridges into other scientific fields: crystalline materials can be turned amorphous by introducing enough defects, such as stacking faults, or other crystallographic manipulation during the precipitation process. A case in point: in Fig. 1, we show an example of how the introduction of acetate ions can create defects during the formation of brucite, which results in a structure similar to that of carbonate-defective brucite in magnesium carbonate cement and gives the material the ability to bind.

Conclusions

Here, we propose an additional factor to the framework of designing cements for improved sustainability.

In the effort to decarbonize the cement industry, solutions to reduce the carbon footprint of cement need to be sustainable by design. By adding the amorphicity of cement hydrates into the design framework, we hope to limit the search space through which one may achieve the required mechanical performance while using less resources and still have the right composition of amorphous phases in the end product. To this end, the inter/trans-disciplinary approach in steering the nucleation and growth of cement hydrates is a powerful tool.

We see high potential in designing novel cements with completely distinct chemistries compared to the conventional ones. This may radically enhance the progress of decarbonizing the industry. Several aspects need also considering, such as the long-term performance of these amorphous phases, the degree of binding capability when the composition of the phases varies, and the availability of the feedstock and the ability to upscale for viable cements. Hereby, we invite the research

community and cement scientists to join forces and take this framework to develop further the portfolio of sustainable-by-nature cements.

Author contributions

HN and PK: conceptualization, writing and revising the manuscript.

Conflicts of interest

There are no conflicts to declare.

Acknowledgements

HN and PK acknowledge funding from the Research Council of Finland project no. 326291 and 329477. HN is grateful for the funding from the Research Council of Finland for Academy Research Fellowship no. 354767. We thank Jasmiini Tornberg for the help in improving the figure presentations, Nirrupama Kamala Ilango for the help with data about acetate-modified brucite, and Ellina Bernard and Barbara Lothenbach for fruitful discussion on MSH and CSH.

Notes and references

- 1 R. M. Andrew, *Earth Syst. Sci. Data*, 2018, **10**, 195–217.
- 2 K. L. Scrivener, V. M. John and E. M. Gartner, *Cem. Concr. Res.*, 2018, **114**, 2–26.
- 3 K. Scrivener, A. Ouzia, P. Juillard and A. Kunhi Mohamed, *Cem. Concr. Res.*, 2019, **124**, 105823.
- 4 B. Pichler and C. Hellmich, *Cem. Concr. Res.*, 2011, **41**, 467–476.
- 5 S. Merlino, E. Bonaccorsi and T. Armbruster, *Eur. J. Mineral.*, 2001, **13**, 577–590.
- 6 E. Bernard and H. Nguyen, *Cem. Concr. Res.*, 2024, **178**, 107459.
- 7 M. Mellini, *Am. Mineral.*, 1982, **67**, 587–598.
- 8 Z. Zhang, Y. Yan, Z. Qu and G. Geng, *Cem. Concr. Res.*, 2022, **159**, 106858.
- 9 E. Duque-Redondo, E. Masoero and H. Manzano, *Cem. Concr. Res.*, 2022, **154**, 106716.
- 10 B. Jönsson, A. Nonat, C. Labbez, B. Cabane and H. Wennerström, *Langmuir*, 2005, **21**, 9211–9221.
- 11 A. Goyal, I. Palaia, K. Ioannidou, F.-J. Ulm, H. van Damme, R. J.-M. Pellenq, E. Trizac and E. Del Gado, *Sci. Adv.*, 2021, **7**, eabg5882.
- 12 Z. Zhang, Q. Zhu and G. Geng, *Composites, Part B*, 2024, **271**, 111140.
- 13 W. Kunther, S. Ferreiro and J. Skibsted, *J. Mater. Chem. A*, 2017, **5**, 17401–17412.
- 14 B. Lothenbach, D. Jansen, Y. Yan and J. Schreiner, *Cem. Concr. Res.*, 2022, **159**, 106871.
- 15 R. J. Myers, E. L'Hôpital, J. L. Provis and B. Lothenbach, *Cem. Concr. Res.*, 2015, **68**, 83–93.



16 S. Grangeon, F. Claret, C. Lerouge, F. Warmont, T. Sato, S. Anraku, C. Numako, Y. Linard and B. Lanson, *Cem. Concr. Res.*, 2013, **52**, 31–37.

17 S.-Y. Yang, Y. Yan, B. Lothenbach and J. Skibsted, *J. Phys. Chem. C*, 2021, **125**, 27975–27995.

18 R. J. Myers, S. A. Bernal, R. San Nicolas and J. L. Provis, *Langmuir*, 2013, **29**, 5294–5306.

19 I. Garcia-Lodeiro, A. Palomo, A. Fernández-Jiménez and D. E. Macphee, *Cem. Concr. Res.*, 2011, **41**, 923–931.

20 E. Bernard, H. Nguyen, S. Kawashima, B. Lothenbach, H. Manzano, J. Provis, A. Scott, C. Unluer, F. Winnefeld and P. Kinnunen, *RILEM Tech. Lett.*, 2023, **8**, 65–78.

21 E. Bernard, *RILEM Tech. Lett.*, 2022, **7**, 47–57.

22 A. German, F. Winnefeld, P. Lura, D. Rentsch and B. Lothenbach, *Cem. Concr. Res.*, 2023, **173**, 107304.

23 E. Bernard, B. Lothenbach, C. Chlique, M. Wyrzykowski, A. Dauzères, I. Pochard and C. Cau-Dit-Coumes, *Cem. Concr. Res.*, 2019, **116**, 309–330.

24 H. Sreenivasan, E. Bernard, H. S. Santos, H. Nguyen, S. Moukannaa, A. Adediran, J. L. Provis and P. Kinnunen, *Cem. Concr. Res.*, 2024, **178**, 107462.

25 D. Jansen, A. German, D. Ectors and F. Winnefeld, *Cem. Concr. Res.*, 2024, **175**, 107371.

26 N. Kamala Ilango, H. Nguyen, A. German, F. Winnefeld and P. Kinnunen, *Cem. Concr. Res.*, 2024, **175**, 107357.

27 F. Winnefeld, E. Epifania, F. Montagnaro and E. M. Gartner, *Cem. Concr. Res.*, 2019, **126**, 105912.

28 F. Winnefeld and B. Lothenbach, *RILEM Tech. Lett.*, 2016, **1**, 10–16.

29 H. Nguyen, P. Kinnunen, K. Gijbels, V. Carvelli, H. Sreenivasan, A. M. Kantola, V.-V. Telkki, W. Schroevers and M. Illikainen, *Cem. Concr. Res.*, 2019, **123**, 105800.

30 J. H. Ideker, K. L. Scrivener, H. Fryda and B. Touzo, in *Lea's Chemistry of Cement and Concrete (Fifth Edition)*, ed. P. C. Hewlett and M. Liska, Butterworth-Heinemann, 2019, pp. 537–584.

31 B. Xu, F. Winnefeld, J. Kaufmann and B. Lothenbach, *Cem. Concr. Res.*, 2019, **123**, 105781.

32 A. Viani, G. Mali and P. Máková, *Ceram. Int.*, 2017, **43**, 6571–6579.

33 B. Lothenbach, B. Xu and F. Winnefeld, *Appl. Geochem.*, 2019, **111**, 104450.

34 M. I. M. Alzeer, H. Nguyen, T. Fabritius, H. Sreenivasan, V.-V. Telkki, A. M. Kantola, C. Cheeseman, M. Illikainen and P. Kinnunen, *Cem. Concr. Res.*, 2022, **159**, 106859.

35 S. Kucharczyk, M. Zajac, C. Stabler, R. M. Thomsen, M. Ben Haha, J. Skibsted and J. Deja, *Cem. Concr. Res.*, 2019, **120**, 77–91.

36 M. B. Haha, K. De Weerdt and B. Lothenbach, *Cem. Concr. Res.*, 2010, **40**, 1620–1629.

37 N. V. Y. Scarlett and I. C. Madsen, *Powder Diffr.*, 2006, **21**, 278–284.

